

Imaging Tree Roots with Borehole Radar

John R. Butnor, Kurt H. Johnsen
USDA Forest Service, Southern Research Station
Research Triangle Park, NC, USA
Email jbutnor@fs.fed.us, kjohnsen@fs.fed.us

Per Wikström
Radarteam AB
Boden, Sweden
Email info@radarteam.se

Tomas Lundmark¹, Sune Linder²
SLU, Swedish University of Agricultural Sciences
Vindeln¹ and Alnarp², Sweden
Email Tomas.Lundmark@esf.slu.se, Sune-Linder@ess.slu.se

Abstract – Ground-penetrating radar has been used to detect and map tree roots using surface-based antennas in reflection mode. On amenable soils these methods can accurately detect lateral tree roots. In some tree species (e.g. *Pinus taeda*, *Pinus palustris*), vertically orientated tap roots directly beneath the tree, comprise most of the root mass. It is difficult if not impossible to vertically delineate these roots with surface-based radars. To address this problem, a collaborative project between the USDA Forest Service, Southern Research Station, Radarteam AB and the Swedish University of Agricultural Sciences (SLU), was undertaken in August 2003 to assess the potential of high-frequency borehole radar to detect vertical, near-surface reflectors (0-2 m) resulting from tree roots. A set of controlled experiments on buried logs were used to test the efficacy of crosshole and borehole to surface travel time data to model near surface woody targets with tomography. Using these results, five *Pinus sylvestris* trees were scanned with borehole to surface radar and tomograms of their root systems were created. Three of the five tomograms compared favorably with root distribution maps made using destructively sampled data. However, the other two trees were misinterpreted, one was sharply underestimated, the other overestimated. This is the first report of using borehole radar to study vertical tree roots. Crosshole tomography provided excellent information on the depth of tree roots, but was less useful for imaging near surface features. Borehole to surface measures provided the best information on the near surface, where the bulk of roots are found (0-0.3 m). The technique has promise in forest research, but the development of new high-frequency borehole antennas, and forward modeling software that allows concurrent processing of travel-time and amplitude data is necessary to further this research.

Keywords – tomography, borehole, crosshole, *Pinus sylvestris*, root mass, root distribution, tree, root, GPR

I. INTRODUCTION

Ground-penetrating radar can be used to detect tree roots provided there is sufficient electromagnetic contrast to separate roots from soil [1]. Forest researchers need root

biomass, distribution and architecture data to assess the effects of forest management practices on productivity and resource allocation in trees. Ground-penetrating radar is a non-destructive alternative to laborious excavations that are commonly employed. Tree roots are not ideal subjects for radar studies; clutter from non-target materials can degrade the utility of GPR profiles. On amenable soils, rapid root biomass surveys provide valuable information in a short period time, though some destructive ground-truthing is required [2]. The location of larger tree roots can be mapped if there is sufficient time for intensive grid sampling. Processing 3D representations of tree roots is computationally intensive, but will become more prevalent as software advances are made to automate these procedures.

Surface-based GPR can provide excellent resolution of lateral roots. However, some forest trees have a significant allocation to large vertical taproots roots (i.e. loblolly pine, *Pinus taeda* L., longleaf pine, *Pinus palustris* Mill.), which cannot be accurately assessed by surface measures. Borehole radar allows investigation of vertically oriented targets and resolution is unaffected by depth. In reflection mode, the transmitter and receiver are lowered into a borehole and an electromagnetic pulse is propagated. The energy moves through the profile until it contacts a region with different electromagnetic properties. A portion of the energy is transmitted back to the receiver in a manner similar to conventional to surface-based radar [3]. In transmission mode, the transmitter and receiver are separated and located in opposite boreholes or placed on the soil surface. By varying the depth or surface locations a variety of ray paths can be created [3]. The simplest variable to measure and model is travel time between the antennas, though accuracy may be increased by monitoring secondary and tertiary arrivals, monitoring amplitude or advanced migration techniques [4]. A collaborative project between the USDA Forest Service, Southern Research Station, Radarteam AB and the

Swedish Experimental Forest system was undertaken in August 2003 to assess the potential of high-frequency borehole radar to detect vertical near surface reflectors (0-2 m) resulting from tree roots.

II. METHODS

2.1 Study Site

This research was conducted near Vindeln in northern Sweden in August 2003. The study site is a naturally regenerated, uneven-aged (50-200 yr) Scots pine (*Pinus sylvestris*) stand located within the Vindeln Experimental Forest (64°14' N, 19° 46' E) in the boreal zone of northern Sweden. The climate is characterized by short growing seasons; the annual mean air temperature is only 1.3 °C. The site lies 180 m above sea level on a flat glacial-luvial plain. The soils are classified as ferric and podzolised and possess a thin humus layer. The sandy soils have eluvial and illuvial horizons which are ~ 10 cm thick and are characterized by low silt and clay contents. The overstory is dominated by Scots pine which are widely spaced. The understory vegetation is sparse and consists of low ericaceous shrubs and lichens. Five trees (*Pinus sylvestris*) whose DBH ranged from 12-37 cm were selected for study.

2.2 Data Collection and Equipment

The objective of this study was to assess the utility of borehole radar to delineate vertical tree roots and the root ball directly beneath a mature tree. At each of five test trees, a 3 m transect was established on the surface. Near the beginning of each transect, a 5 cm soil auger was used to bore to a depth of 2.5 m, the subject tree was located at the midpoint (1.5 m) and another borehole was located at the end of the transect (3 m). This configuration allowed for reflective measures from a single hole, travel time measurements between holes and borehole to surface measures. We used a 1000 MHz borehole transducer (Tubewave-1000, Radarteam AB, Boden, Sweden) along with a GSSI Sir-20 ground-penetrating radar unit (Geophysical Survey Systems Inc., North Salem, NH, USA) to collect reflective data in boreholes adjacent to trees (Figure 1). At the time of the experiment, only one TW-1000 was available. In order to make travel time measurements we configured the TW-1000 as a transmitter (Tx) and used a GSSI 900 MHz antenna configured as a receiver (Rx). This worked very well for the purposes of this study, the center frequencies of the antennas were well matched; however the dimensions of the 900 MHz antenna required us to dig a larger hole to effectively lower the Rx antenna opposite the Tx antenna. Tx was operated in single shot mode, where an electromagnetic pulse was propagated and the time it took to penetrate the soil matrix and be detected by the Rx on the opposite side of the tree was measured.



Figure 1. GSSI Sir-20 radar unit, 900 MHz antenna (left) and TubeWave-1000 (right) on opposite sides of Scots pine tree.

To allow for tomographic reconstruction of the vertical roots, a series of crosshole rays were created by raising and lowering the antennas at intervals of 5 cm. Then the antennas were moved to opposite holes and the process was repeated creating 1152 unique travel-paths per tree (Figure 2).

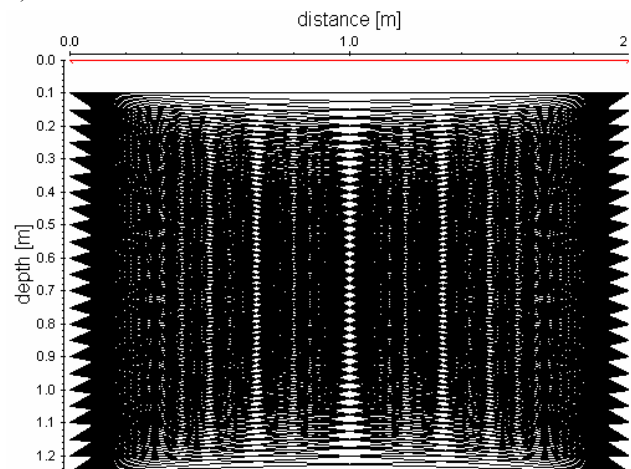


Figure 2. Crosshole ray diagram, showing 1152 unique paths.

Borehole to surface measures were collected in a similar fashion, though the Rx was moved across the soil surface (10 cm interval) and the Tx was manipulated below ground (5 cm interval), generating 2400 travel-paths per tree (Figure 3). The travel-time data sets were combined to create a master set composed of 3552 observations. We decided to limit the crosshole measures to a depth of 1.25 m to maximize overlap with the borehole to surface measures and judiciously reduce the number of manually collected observations.

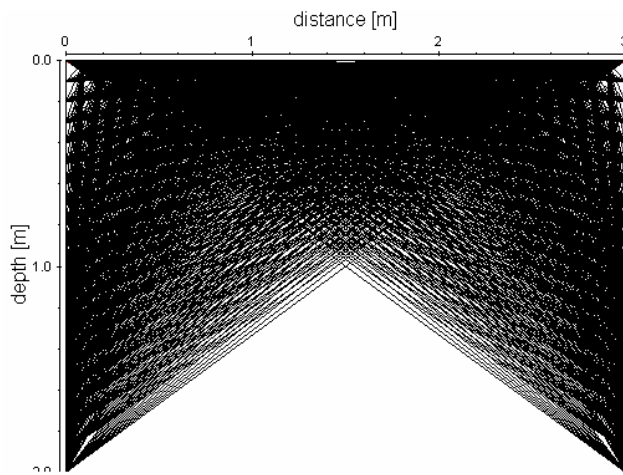


Figure 3. Borehole to surface ray diagram, showing 2400 unique ray paths

2.3 Testing Methodology

A trial run was conducted to test the sampling methods using an “artificial” tap root. Instead of a tree at 1.5 m on the transect, a large diameter soil auger was used to bore a hole to 0.8 m and a fresh cut Scots pine log (27.5 cm diameter) was inserted. Only borehole to surface measures were collected. The log was removed and a shorter log segment (40 cm) was inserted to a depth of 0.8 m and the hole was filled with soil. Both crosshole and borehole to surface measures were made. This configuration allowed a more complete delineation of the cut log since electromagnetic pulse could pass directly over the top of the target.



Figure 4. Preparing to bury a fresh cut log sections .

2.4 Data Processing and Tomography.

All data processing and modeling was performed using REFLEXW Version 3.0 (K.J. Sandmeier, Karlsruhe, Ger-

many). The raw data consists of travel time values and amplitudes. Version 3.0 of REFLEXW was designed to allow for tomographic modeling of travel time transmission and reflection data from GPR, ultrasound or seismic sources. It did not permit the interpretation of signal strength or amplitude in tomographic modeling mode [5]. For our study, we used the first time of arrival of the propagated electromagnetic signal and ignored any secondary or tertiary arrivals which may have taken a more circuitous path than those in the ray diagrams (Figures 2 and 3). It was necessary to create a “pick” file which determines the first arrival time for a given ray and compile this data to be interpreted by the tomography model. A number of different analysis models were attempted to interpret the travel time data. The best agreement was found with simple beam and weighted beam models. Use of curved ray models seemed to over-migrate, accurately showing the location of the object, but not size or proper shape. The end result of forward modeling was a tomogram which represents the physical properties of a two dimensional plane between the boreholes [5]. The success of this study was dependent on the tree roots having distinct electromagnetic contrast against the fine sandy soil.

2.5 Destructive Harvest of Root Systems

After the five trees were scanned with GPR, the orientation of the transect was marked on the trunk for future reference. The trees were removed from the soil using a specially designed winch system; wherein a cable was placed 15 + m up the tree and the leverage of the bole was used to topple the tree. Near the base of the tree at breast height a triangular bumper was affixed and served as a fulcrum to help dislodge the root ball without breaking the roots. Technicians at the Vindeln Experimental Forest removed the root ball and used a pressure washer to remove any remaining soil. In order to quantitatively assess the root characteristics of each tree, a strategy was devised to assess and spatially differentiate root mass. Roots directly between the boreholes likely had the greatest influence on EM travel-time, but there was no available guidance on the width of the detection zone. Based on preliminary findings with the buried root tests, we sampled 0.25 m on either side of the transect and discarded any roots outside of this area (Figure 5). The potential root volume beneath the measurement footprint (Figure 5) was differentiated by depth and distance along the transect. As roots were sampled, they were assigned a cell number which corresponds with the diagram in Figure 6. The roots were oven dried at 55 °C for several weeks and weighed; no root size class information was collected. It was necessary to develop a projection of the root mass data between the two boreholes to compare with the tomograms. This could be achieved in a rudimentary fashion by using the 15 cells (Figure 6) versus the 100,000+ pixels in each tomogram. Instead, a modeling technique which migrated the mass of each cell

towards the tree center or nearest concentration of root mass, to differentiate the likely distribution of mass within the cell. This was achieved by sub-dividing each cell into 9 equal sized units with the identical value and running a contour analysis in SigmaPlot 2001 (SPSS, Inc.).

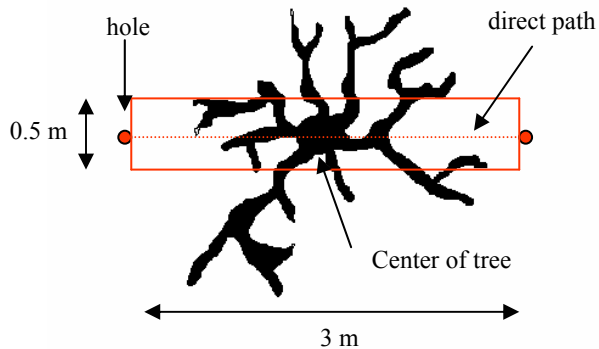


Figure 5. Aerial view of root sampling area, only roots within lines (0.5 m X 3.0 m) were collected.

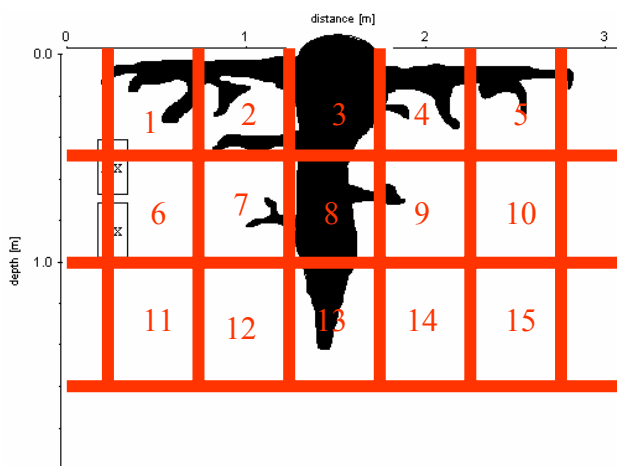


Figure 6. Diagram depicting the root mass cell matrix; each root mass cell was 0.5 m X 0.5 m X 0.5 m.

III. RESULTS

3.1 Buried Log Tests

Initial work with TW-1000 in reflection mode was difficult to interpret. Much like surface-based high frequency GPR, reflectors close to the antenna were well defined, but resolution was limited by horizontal penetration. This was problematic when scanning near the base of a large tree with many interconnected roots. We did not have access to pulley mounted survey wheel which would have made the metering of pulses more accurate. The use of reflection borehole GPR was discontinued and the focus was placed on crosshole and borehole to surface measures.

The crosshole data modeled with REFLEXW accurately defined the vertical limits of the 0.4 m buried log (Figure 7A), demonstrating that the fresh cut log is a suitable target for GPR in this soil type. The horizontal location of the log along the transect was not resolved with crosshole tomography. The crosshole measurements were collected to a depth of 1.25 m, which is deeper than most roots would penetrate. However, when the Rx and Tx were offset vertically there were few ray paths that were unaffected by the position of the log; only those with minimal slope could trace the margins of the target.

The borehole to surface data created a tomogram which effectively located the buried log along the horizontal plane (Figure 7B), yet was less capable of defining the vertical margins of the log. Figure 7B, shows a bias towards the right side of the tomogram which seems to pull the predicted location of the log to the right. It is not known if there were any other reflectors inducing clutter near the bottom of the borehole, but it would be unlikely in this soil. Other explanations include: poor transmission from the bottom of the borehole to the furthest extent of the transect, the bottom of the log may have been slightly tipped, presenting a more resistive surface to the EM pulse, or the soils on the right side of the diagram exhibited different electrical properties which affected the EM travel time. When the data sets were combined there was a moderation of the biases noted in the individual data sets (Figure 7C). The depth of the buried log is more accurate than using the borehole to surface data alone. The bias towards the right side of the diagram remains, but is minimized.

The 1.2 m log (buried to 0.8 m) was intended to simulate conditions as would be found with large vertical tap roots, with the caveat of not having direct Rx access to the surface where the log protrudes from the ground. Considering the results of the 0.4 m log test, and the time required to manually collect thousands of single shot EM transmissions, only borehole to surface data were collected. The resulting tomogram approximated the shape of the 1.2 m log (Figure 8), though similar to the 0.4 m log test (Figure 7B), there was a strong bias to the borehole on the right. Both log lengths were measured using the same auger hole and boreholes, so any soil effects would be similar. The modeled log in Figure 8 shows some distortion near the surface creating a cross-shaped pattern, which was not observed in the previous test. Shallow soil depth combined with the log protruding from and disrupting the soil surface may be reducing the quality of the signal transmission. The effect is exaggerated by the lack of 7-8 ray paths which cannot be sampled due to the protruding log.

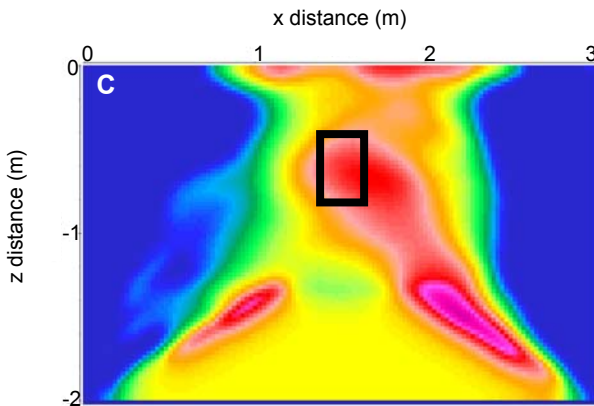
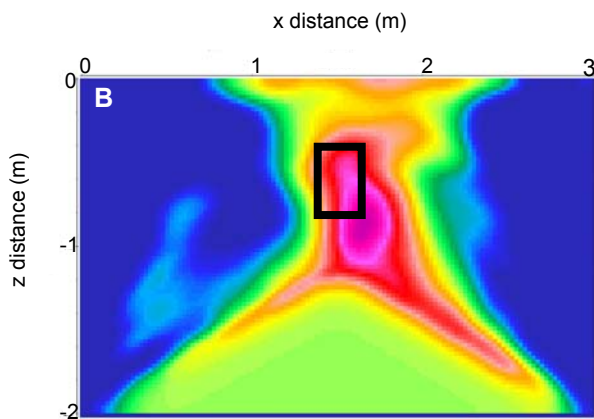
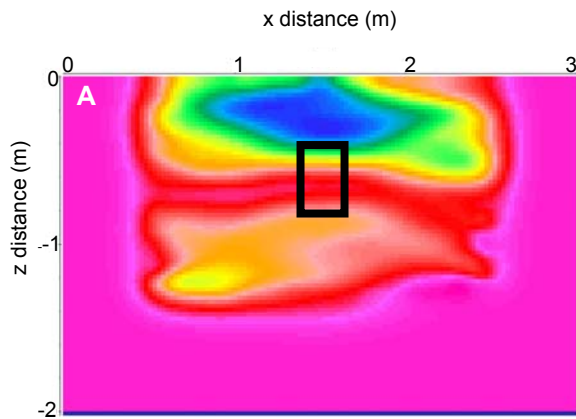


Figure 7. Tomograms from the 0.4 buried log test m (actual location marked in black) modeled using A) crosshole only data, B) borehole to surface data and C) combined crosshole and borehole to surface data ($x=0$ to 3 m, $z=0$ to -2 m).

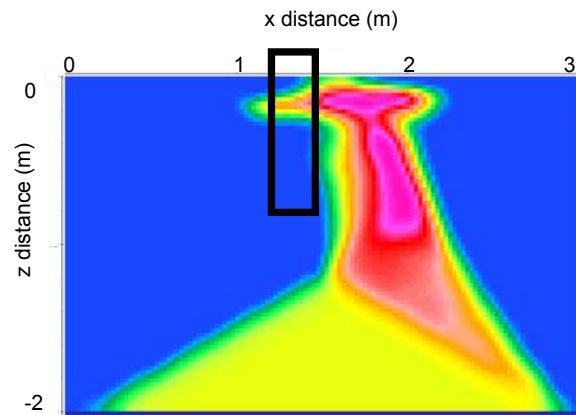


Figure 8. Tomogram from the 1.2 m buried log test m (actual location marked in black) modeled using borehole to surface data ($x=0$ to 3 m, $z=0$ to -2 m).

3.2 Tree Analysis

Each of the trees was scanned using the borehole to surface sampling scheme in Figure 3, and modeled with REFLEXW to produce the tomograms in Figure 9. The array of model options in reflex are quite extensive [5]. Some level of interpretation was required to choose the model parameters, but we had the benefit of the buried log of known dimensions to help parameterize the model. The model derived from the buried log tests was applied to all five trees. This was performed without prior knowledge of the destructive harvest data. Root mass collected by destructive sampling, and divided into 15 cells, was modeled to show the spatial distribution of mass and project a rooting area map on the 4.5 m² plane ($x=0$ to 3 m, $z=0$ to -1.5 m) between the boreholes (Figure 9). Trees 1, 2 and 4 display a high degree of similarity between the tomograms and the root maps (Figure 9). Tree 1 shows a large mass beneath the bole, extending to either side. Directly underneath the tree is a region where root density is noticeably reduced. Tree 2 is the smallest tree, having only 5.1 kg of roots in the sampling zone (Table 1). The tomogram clearly shows that this tree has the smallest root ball and limited rooting area within the measurement plane (Figure 9). There is a bit of clutter in the tree 4 tomogram, the contours originating from the lower right side, rising to meet the root ball, will be removed from additional analysis. Otherwise, this is also a good match. Trees 3 and 5 appear to be misinterpreted by the tomogram. Tree 3 is the second smallest tree, though the tomogram shows a relatively large rooting area on the xz plane (Figure 9). The opposite condition is observed with tree 5; this large tree is interpreted as having a much smaller root ball than was found destructively.

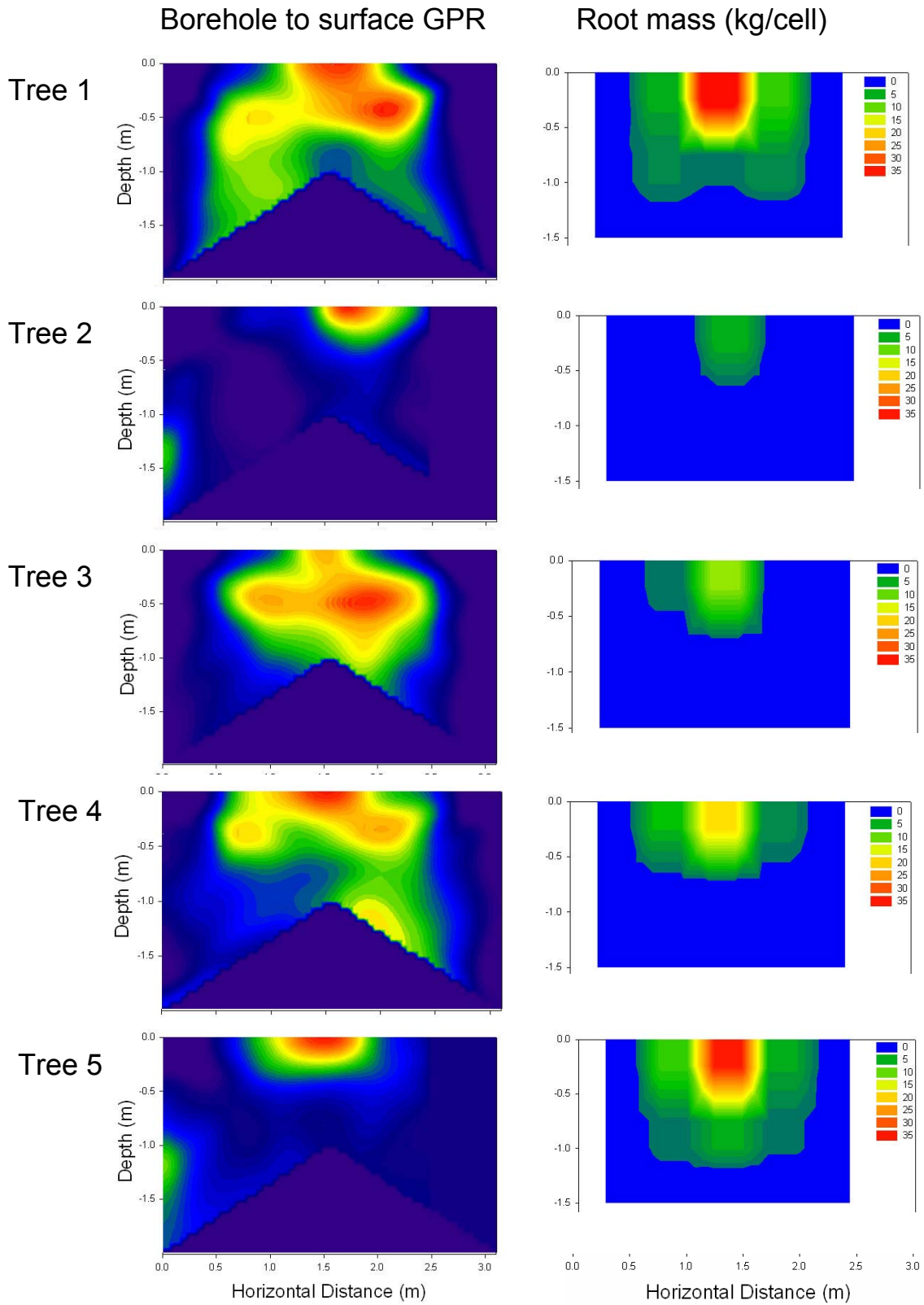


Figure 9. Comparison of borehole to surface tomography and the model of actual root mass ($x=0$ to 3 m, $z=0$ to -2 m).

Table 1. Root mass within the sampling area, diameter at breast height (DBH) and age of the five study trees.

Tree #	Root mass (kg)	DBH (cm)	Age (yr)
1	60.5	36.7	193
2	5.1	12.1	56
3	13.6	18.7	71
4	26.4	23.5	110
5	55.1	32.5	191

In order to quantitatively compare data derived from GPR and the destructive sampling, we compared the rooting area contour map created with SigmaPlot using root mass linked to spatial distribution among the cells to the total root mass harvested from each tree (Table 1). The projected rooting area on 4.5 m² plane between the boreholes was highly correlated to total root mass (Figure 10). It must be noted that these variables are co-related; projected rooting area is derived from the root mass in each cell. However, this does demonstrate that projected rooting area is a function of total root mass and can be used for comparison with the tomograms.

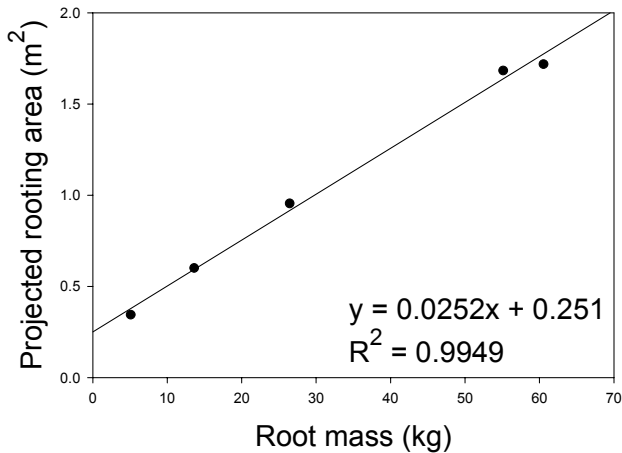


Figure 10. Projected rooting area in the 4.5 m² plane between the boreholes (x =0 to 3m, z=0 to -1.5m) compared to total root mass.

The relationship between projected rooting area and radar derived rooting area is rather poor (Figure 11). This is due to the misinterpretations of trees 3 and 5.

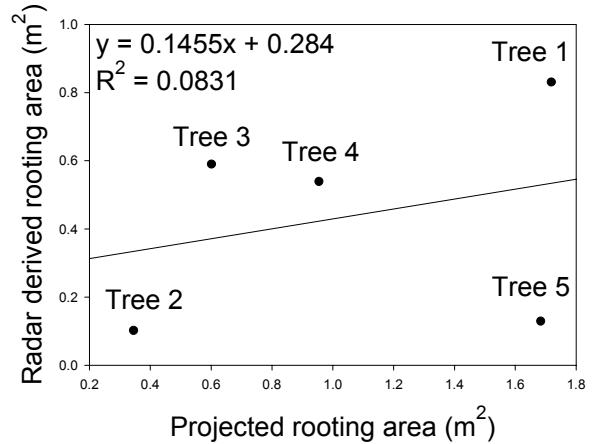


Figure 11. Projected rooting area compared with radar derived rooting area.

The application of simple allometry, which relates the relative size or growth of an easily measured tree parameter (e.g. diameter at breast height) to a parameter which is more difficult to directly sample, in this case total root mass is still superior to borehole radar results (Figure 12).

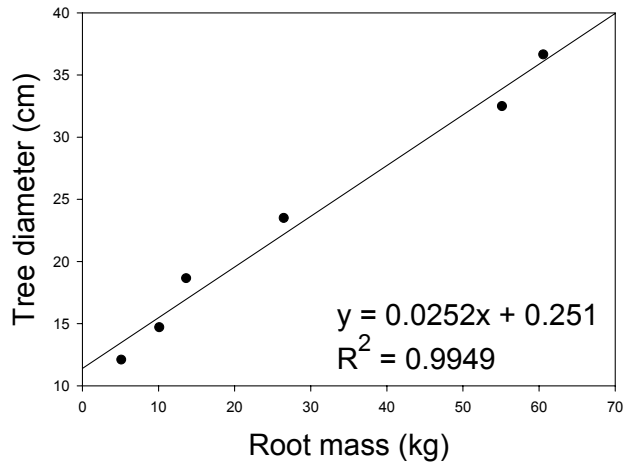


Figure 12. Comparison of tree diameter at breast height to root mass in the measurement area.

IV. DISCUSSION

This is the first report of using borehole radar to study vertical tree roots. Cross-hole tomography provided excellent information on the depth of tree roots, but was less useful for imaging near surface features. For crosshole tomography to successfully image tree root structures, the boreholes need to be deep enough to achieve the pitch necessary to resolve the mass of roots near the surface. In the case of the 0.4 m buried log, few, if any, ray path travel

times were unimpeded by the presence of the log. Borehole to surface measures provided the best information on the near surface, where the bulk of roots are found (0-0.3 m). This new application of borehole GPR worked very well on 3 of 5 trees, but clearly misinterpreted the other two trees. Based on the buried log tests, overestimation is more likely when there is a flat reflective surface at an oblique angle to the ray path, as in the case of the cut end of the buried log. Overestimation may also occur if there is a degradation of the wall of the borehole, preventing adequate contact for penetration. This is important on near surface studies where borings are in soil versus solid rock. The causes of root mass underestimation are less obvious.

Forward modeling of borehole data using REFLEXW version 3.0 software was limited to travel-time data. Inclusion of amplitude forward modeling would likely enhance mass quantification. The addition of secondary and tertiary arrivals would also help refine the interpretative value of the data [4]. It was possible to “pick” arrival times other than the first arrival in REFLEXW, however it was a manual process demanding a user to select the individual data points [5]. Considering the thousands of transmissions collected and the potential for arbitrary arrival time assignments, this was not a viable processing option.

Borehole radar has promise in forest research, but the development of new high-frequency borehole antennas, and forward modeling software that allows concurrent processing of travel-time and amplitude data is necessary to further this research. We had hoped to find *P. sylvestris* trees exhibiting well defined vertical tap roots, instead many smaller vertical roots (< 1 m) deep comprising a large “root ball” were observed. It may be valuable to use this technology to measure tap root depth in deeply rooted *Pinus palustris* trees. This would be useful to estimate below-ground carbon storage in living tree organs and better understand where they acquire resources deep within the soil profile.

The Tubewave-1000 was not designed specifically for this study or for root analysis. In 2005, an improved version of the Tubewave-1000 became available; featuring a new non-dipole configuration and more sensitive Rx/Tx electronics. It could be refined to permit wave propagation from a smaller point-source, to resolve smaller targets and more accurately define the origin of the transmission. This study used extremely small sampling intervals (5 and 10 cm) which would benefit from these changes. Automation of data collection would also enhance the utility of borehole methodology. The time required to sample each tree manually was 5-6 hours. The development of self contained winch-based survey wheels, modular tracks upon which antennas could be moved on the surface and soft-

ware to choreograph the antenna movements and measurements would revolutionize the applied use of this technology.

Presently allometry gives more accurate estimates of root mass than travel-time tomography, however allometric relationships are typically site and species dependent. Considerable amounts of destructive sampling are needed to parameterize equations for a given site. When experiments are conducted which alter carbon assimilation or allocation in trees, standard allometric equations cannot be assumed valid.

V. CONCLUSIONS

Borehole radar has promise in forest research, but the development of new high-frequency borehole antennas, automated data collection systems and forward modeling software that allows concurrent processing of travel-time and amplitude data is necessary to further this research.

ACKNOWLEDGMENTS

This research was supported by the USDA Forest Service, Southern Research Station, and the Swedish University of Agricultural Sciences (SLU). The technical assistance in the field was provided by Tomas Hörnlund, Otilia Johansson and Ludwig Dorfstetter. RadarTeam AB graciously provided the equipment used in this study as well as technical support (www.RadarTeam.se).

REFERENCES

- [1] Butnor, J.R., J. Doolittle, L. Kress, S. Cohen, and K.H. Johnsen. 2001. Use of ground penetrating radar to study tree roots in the southeastern United States. *Tree Physiology*, 21, 1269-1278.
- [2] Butnor, J.R., J.A. Doolittle, K.H. Johnsen, L. Samuelson, T. Stokes, and L. Kress. 2003. Utility of ground-penetrating radar as a root biomass survey tool in forest systems. *Soil Science Society of America Journal*, 67, 1607-1615.
- [3] Wänstedt, S., S. Carlsten, and S. Tirén. 2000. Borehole radar measurements aid structure geological interpretations. *Journal of Applied Geophysics*, 43, 227-237.
- [4] Zhou H. and M. Sato. 2004. Subsurface cavity imaging by crosshole borehole radar measurements. *IEEE Transactions on Geoscience and Remote Sensing*, 42, 335-341.
- [5] Sandmeier, K.J. 2003. REFLEXW Version 3.0 for the processing of seismic, acoustic or electromagnetic reflection, refraction and transmission data. 346p. contact www.sandmeier-geo.de for availability.